

Synthesis and characterization of a series of conducting polymers based on indole and carbazole

Mehmet ERGİNER, Belkis USTAMEHMETOĞLU^{ORCID}, Esmâ SEZER*^{ORCID}

Department of Chemistry, İstanbul Technical University, İstanbul, Turkey

Received: 05.02.2022 • Accepted/Published Online: 10.08.2022 • Final Version: 05.10.2022

Abstract: A series of indole (In) and carbazole (Cz) derivative monomers have been synthesized, such as 4-[3-carbazolyl] indole (4In-3Cz), 5-[3-carbazolyl] indole (5In-3Cz), 6-[3-carbazolyl] indole (6In-3Cz), 7-[3-carbazolyl] indole (7In-3Cz). The comonomers synthesized by Stille coupling reaction were characterized by ¹H-NMR and elemental analysis. Potentiodynamic method was used for electropolymerization of comonomers, Indole, Cz, and the mixture of In and Cz. Electrochemical activities of resulting P[4In-3Cz], P[5In-3Cz], P[6In-3Cz], P[7In-3Cz], polyindole (PIn), polycarbazole (PCz) and P[In-co-Cz] films were investigated comparatively by CV at different scan rates, electrochemical impedance spectroscopy (EIS) and spectroelectrochemical measurements. The ionization potentials, I_p , specific capacitance, C_{sp} , and optical band gap, E_g , of copolymers were obtained from these measurements. In order to gain some preliminary information on the structure of the copolymers, DFT analysis was performed and dimers and tetramers were optimized.

Results suggested that, in order to obtain an In-Cz copolymer with low oxidation potential and band gap, indole ring should be substituted through 5 position to the 3 position of Cz. If high specific capacitance value or high conductivity are desired, P[4In-3Cz] and P[6In-3Cz] are the best copolymers, respectively.

Key words: Carbazolylindoles comonomers, synthesis, electropolymerization, electronic and optical properties

1. Introduction

There has been a great deal of interest recently in the development of organic-based materials for the applications in the electronics industry. Although less studied than other families of conducting polymers, PCz derivatives could be used in electroluminescent devices as a hole-transporting material, in field effect transistors, batteries, as biosensor, as a light emitting material or a wide band gap energy transfer donor and for other applications [1-3]. Relatively stable radical cations (holes) those easily forms, relatively high charge carrier mobilities, possibility of easy introduction to different substituents, high thermal and photochemical stability, being a cheap raw material, which is readily available from coal tar distillation makes PCz favorable for such applications.

Although PIn has lower electroactivity than other conducting polymers, in recent years due to its important potential in various areas, such as batteries, electronics, sensors, and corrosion protection, it has attracted a significant amount of attention [4-10].

To improve the properties of PIn, electrochemical copolymerization with pyrrole [11,12], thiophene [13] and derivatives [14] and carbazole [15-17] has been explored in the literature. The results showed that these new copolymer materials can offer improved electrochemical activity and stability and better mechanical properties, thereby increasing the application possibilities [18-22].

Another method of obtaining copolymers with desired repeating unit is coupling reactions. While there are a lot of studies on the synthesis the indolocarbazole alkaloids that have indolo[2,3-*a*] Cz as a structure [23-25], studies on substitution of carbazole to benzene ring of indole are less common although it might be electrochemical activity that makes it a good candidate for various applications.

Synthetic methods such as Stille, Yamamoto, Kumada, and Suzuki couplings that led to obtain alternative copolymers with desired properties and improved performance were utilized recently [26-41] and structure-property relationships of result materials can be understood better. Copolymers obtained by these methods exhibit very low optical band gap and switch between different colors, which is potentially useful for electrochromic devices [42]. In the previous work some

* Correspondence: esezer@itu.edu.tr

indoles have been prepared in one step by adding suitable organometallic reagents, followed by LiAlH_4 to a refluxing mixture of isatin in ether [43]. However, in this study, indole was substituted through the 2-position which limits the polymerization possibilities of indole ring.

In the literature, there are some studies on the synthesis of heteroaryl and allylindoles by Stille cross-coupling reactions [44] that offer advantages to the Suzuki reactions in view of the neutral conditions and the stability and accessibility of the tin derivatives.

Previously, we have also synthesized 5-(2-thienyl) indole (5In-2Th) comonomer [39] and Th-, Cz-, and thiazole-based monomers by using Stille cross coupling reaction [37, 40, 41].

Although there have been previous studies on the synthesis of indole and Cz comonomers with other monomers, studies on the synthesis of In-Cz comonomers are outside of our knowledge. In this study, 4In-3Cz, 5In-3Cz, 6In-3Cz, and 7In-3Cz were synthesized, polymerized, and comparatively characterized for the first time. Their physical properties were obtained by spectroscopic and electrochemical techniques. The results showed that P[4In-3Cz], P[5In-3Cz], P[6In-3Cz], P[7In-3Cz] are promising for applications as they have lower oxidation potentials and optical band gaps than homopolymers.

2. Experimental

2.1. Materials

Analytical grade chemicals of the highest purity, such as acetonitrile (ACN) and dichloromethane (CH_2Cl_2), sodium perchlorate (NaClO_4), In, Cz, tetramethyl ethylene diamine (TEMED), trimethyl tin chloride ($\text{Sn}(\text{CH}_3)_3\text{Cl}$), MgSO_4 , trans-dichloro bis-triphenyl phosphine palladium (II) ($\text{Pd}(\text{PPh}_3)_2\text{Cl}_2$), *tert*-butyl lithium (*t*-BuLi), K_2CO_3 , 4-chloro-indole (4-ClIn), 5-bromo-indole (5-BrIn), 6-chloro-indole (6-ClIn), 7-chloro-indole (7-ClIn), were used as supplied. Toluene and tetrahydrofuran (THF) were dried over sodium before use. All preparations and reactions were performed by using standard Schlenk line techniques under a N_2 atmosphere.

3. Measurements

NMR spectra were collected on a Bruker 250 MHz spectrometer and referenced to the residual proton solvent resonance. CHNS-932 LECO model device was used for elemental analysis.

ATR-FTIR measurements were performed with Perkin Elmer spectrum one spectrophotometer.

Keithley 2400 model multimeter connected to Lucas labs 302 model probe holder and SP4-180-TFS type probe was used to measure solid state electrical conductivity of polymers from pellets with a thickness of 0.8 mm. The following equation was used for calculation [45, 46]:

$$\sigma = V^{-1} I (\ln 2 / \pi d_n)$$

where σ = conductivity, V is the potential in volts, I is current in ampere, and d_n is the thickness in cm which was measured by using a digital caliper.

PARSTAT 2263 model potentiostat/galvanostat controlled with Power Suite software via a computer was used for electrochemical polymerization and characterization. Measurements were performed in a three-electrode cell that contains a Pt button (area of 0.02 cm^2), Pt wire, and Ag wire as the working, auxiliary, and reference electrode, respectively. Calibration of pseudo-reference was performed externally by using a 5 mM ferrocene/ferrocenium solution that has a potential 0.35 V vs. Ag/AgCl. Spectroelectrochemical measurements were performed by Shimadzu 160A model UV-visible spectrophotometer in a quartz cell. Indium tin oxide (ITO) coated glass electrode with a size of $7 \text{ cm} \times 5 \text{ cm} \times 0.11 \text{ cm}$ that has a resistivity $R \leq 12 \Omega / \text{cm}$ obtained from Colorado Concept Coatings Company was used as working. Pt wire and Ag wire were counter and a reference electrode, respectively. Capacitive behavior of polymers was tested by electrochemical impedance spectroscopy (EIS) measurements that performed in the range of $10 \times 10^3 \text{ Hz} - 10 \times 10^{-3} \text{ Hz}$ with 10 mV amplitude at open circuit potential.

Density functional theory (DFT) method at 6-31g* level was used for optimization of comonomer and oligomer geometries. Gaussian software [47] was used for the calculations on the supercomputer of High-Performance Computing Center at ITU.

4. Synthesis

In-Cz comonomers were synthesized by Stille coupling reactions between haloindoles and 3-trimethyl tin Cz which was synthesized by the reaction of Cz and $\text{Sn}(\text{CH}_3)_3\text{Cl}$.

i) Synthesis of 3-(trimethyl stannyl)carbazole

Firstly, a 100-mL Schlenk flask equipped with a stirring bar and N_2 inlet/outlet was dried and charged with ~80 mL of THF, 2.00 g (12 mmol) of Cz, and 1.39 g (12 mmol) of TEMED. After cooling the flask to -78°C , 2.5 M (12 mmol) *t*-BuLi

in hexanes was added and stirred at this temperature for 1 h. Then, 2.39 g (12 mmol) of Sn(CH₃)₃Cl in 15 mL of THF was added dropwise. The mixture was stirred overnight at room temperature. After evaporation of solvent under vacuum, 100 mL of CHCl₃ was added to the mixture. The extraction of product from solution was performed by CHCl₃ and washing with water. Organic phase was collected dried by MgSO₄. The solvent was evaporated under vacuum and a dark yellow product was obtained. The product was characterized with ¹H NMR and FT-IR measurements.

(Yield = 1.3 g, 74%). ¹H NMR (in CDCl₃): δ (ppm) (8.1, 2H, dd), 8.0 (1H, s), 7.6-7.4 (4H, m), 7.2 (1H, s), 0.34 (9 H, s)

In the FT-IR spectrum, the presence of -N-H str. at 3412 cm⁻¹, aliphatic -C - H str. of trimethyl group at 1935-1695 cm⁻¹, -C = C aromatic ring str. at 1625-1411 cm⁻¹, -C - Sn str. at 1090-996 cm⁻¹, -C - Sn out of plane deformation at 798 cm⁻¹, supported the synthesized Sn-Cz structure.

ii) Synthesis of carbazoyl-indole comonomers

Firstly, 7.65 mmol (2.86 g) 4-bromo indole, 7.65 mmol (1.5 g) 3-trimethyl stannyl carbazole, and 0.3 mmol (0.012 g) trans-dichloro bis triphenylphosphine palladium (II) chloride in 100 mL of toluene solution was prepared and reaction was continued for 24 h under reflux.

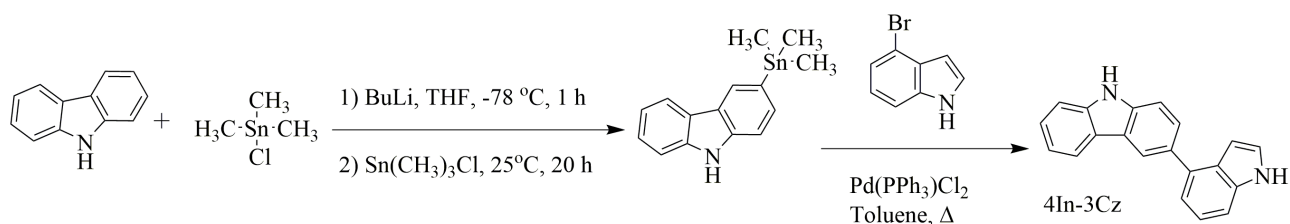
At the end of the reaction, mixture was poured into water and extracted with CH₂Cl₂. The process was repeated three times and the organic phases were combined and dried with K₂CO₃. After evaporation of some solvent, purification of the product was carried out by flash chromatography that contains silica gel as a stationary phase and CHCl₃/hexane/THF; 1:1:1, v/v mixture as eluent.

Synthetic route and the structures of synthesized comonomers are shown in Schemes 1 and 2, respectively.

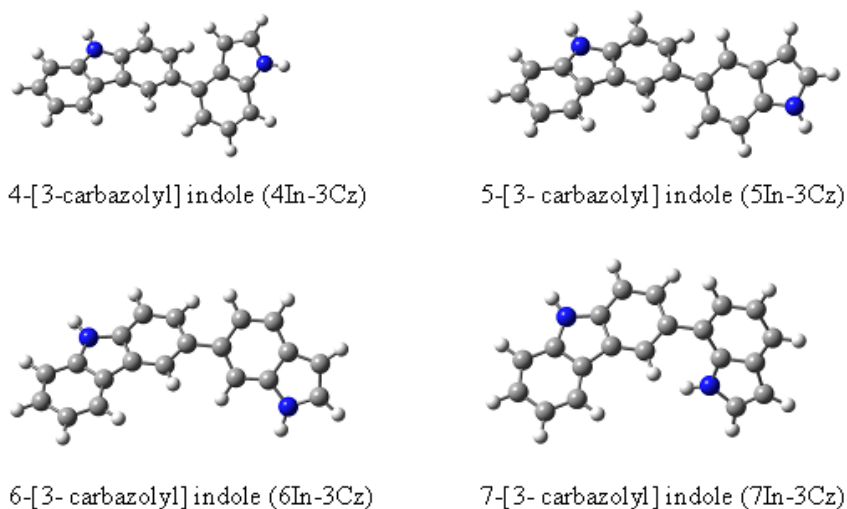
Comonomers were fully characterized by ¹H-NMR and elemental analyses and results are given below. Observation of all numbered protons (inset) of 4In-3Cz comonomer, as an example, given in ¹H-NMR spectrum, supported the synthesis of comonomers (Figure 1).

The yields and the elemental analysis of the comonomers are given below:

4In-3Cz Yield: %50. Elemental analysis: C: 85.6%, H:6.3%, and N:7.9%. ¹H-NMR: (250 MHz, in CDCl₃) (δ, ppm); 6.45 (H3) 7.1-7.00 (H2, H5), 7.20-7.30 (H6, H7, H9, H14), 7.4-7.5 (H10, H12, H13), 8.05 (H11, H15, H16), 8.15 (H1).



Scheme 1. Synthesis of 3-(trimethyl stannyl) carbazole and 5-[3-carbazoyl] indole.



Scheme 2. Structure of In-Cz comonomers.

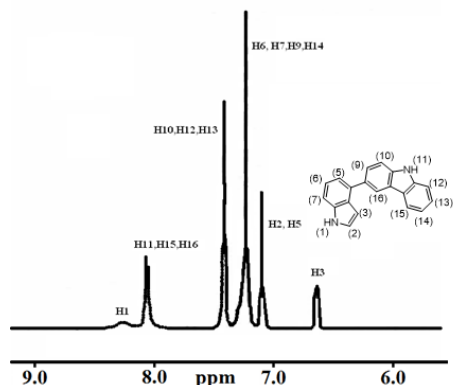


Figure 1. $^1\text{H-NMR}$ Spectrum of 4In-3Cz. Protons of 4In-3Cz comonomer (inset).

5In-3Cz Yield: 40%. Elemental analysis: C: 85.12%, H: 4.96%, N: 9.3%. $^1\text{H-NMR}$: (250 MHz, in CDCl_3): (δ , ppm); 6.50 (H3) 7.0-7.25 (H2, H6, H7, H14), 7.4-7.5 (H9, H10, H12, H13), 7.6(H4), 7.81 (H1), 8.03 (H11), 8.10 (H15, H16).

6In-3Cz Yield: 47%. Elemental analysis: C: 84.74%, H: 5.9%, N: 7.871%. $^1\text{H-NMR}$: (250 MHz, in CDCl_3): (δ , ppm); 6.52 (H3), 7.05(H2), 7.12(H5), 7.24(H14), 7.27(H7), 7.40-7.45 (H9, H10, H12, H13), 7.64 (H4), 7.83 (H1), 8.05 (H11), 8.16 (H15, H16).

7In-3Cz Yield: 57%. Elemental Analysis: C: 85.47%, H: 5.03%, N: 8.82%. $^1\text{H-NMR}$: (250 MHz, in CDCl_3): (δ , ppm); 6.47 (H3), 7.05(H2), 7.12(H5), 7.18(H6), 7.24(H14), 7.42-7.48 (H9, H10, H12, H13), 7.64 (H4), 7.81 (H1), 8.04 (H11), 8.09 (H15, H16).

Elemental analysis results of comonomers agreed with theoretical ones; C: 85.71 %, H: 4.29 %, N: 10.00 %. These results suggested that the comonomer structure contains one Cz unit for one indole unit.

4.1. Electropolymerization

The electropolymerization was performed in 0.1 M NaClO_4 containing ACN on Pt by potentiodynamic method in the potential range of -0.2 V (vs. SCE) up to 1.8 V at 20 mV s^{-1} . Different cycle numbers were applied during electropolymerization to obtain polymer films at different thicknesses and optimum thicknesses were determined according to the redox behaviors.

For comparison, random copolymer of indole and Cz was also prepared starting from their mixtures under the same conditions and called P[In-co-Cz]. The exact concentrations of pristine monomers (Cz, In, and In-Cz comonomer) were 1.0×10^{-3} M and the total concentration in the mixture of In and Cz was also 1.0×10^{-3} M by using 0.5×10^{-3} M In and 0.5×10^{-3} M Cz.

All polymeric films were washed with ACN before characterization.

4.2. Voltametric measurements

Electrochemical oxidation onset potentials (E_{ox}) from CVs were obtained at the position where the current starts to increase. Figure 2A shows the first anodic scan of CVs for In, Cz, In + Cz mixture, and 4In-3Cz and their E_{ox} values were determined from this figure as 1.14, 1.24, 1.16, and 1.06 V, respectively. The mixture of In and Cz has a current value that is between what In and Cz individually have, as expected. A solution containing 1.75×10^{-4} M 4In-3Cz showed lower E_{ox} than the others and the current value was the highest. This result suggested that the 4In-3Cz behaved differently than the mixture of In and Cz, which supported the formation of comonomer. When the polarization curves of comonomers were compared, it can be seen that the E_{ox} values were close to each other and current intensities at maximum peak potentials were shifted and 6In-3Cz has the lowest value (Figure 2B).

Ionization potential (I_p) was calculated as suggested in the literature [48]:

$$I_p = E_{\text{ox}} + 4.4 \text{ (eV)} \quad (1)$$

E_{ox} and calculated I_p values of monomers are summarized in Table 1.

The results suggested that it is possible to obtain new comonomers by cross-coupling reactions of Cz and In with lower oxidation potential than the value of starting monomers.

In, Cz, and In + Cz were polymerized potentiodynamically, and electroactivities of the polymers were tested by CV performed at variety of scan rates and results are illustrated in Figure 3.

Oxidation started at 1.14 V, 1.24 V, and 1.16 in the first scan of In, Cz, and In + Cz, respectively, which were attributed to formation of cation radicals by oxidation of the monomers (Figures 3a–3c). In the first cycle, when potential up to 1.4 V is applied for In + Cz similarly with the polymerization of In and Cz, a faster current increase was observed after the peak potential of around 1.1 V. For this reason, the applied potential has been reduced to prevent overoxidation of the copolymer film formed on the surface, which has lower redox activity (Figure 3c). In the following cycles, a new peak appeared at lower potentials, 0.62 V (E_{p1}), 0.87 V (E_{p1}) and 0.52 V (E_{p1}), 0.93 V (E_{p2}) for In, Cz, and In + Cz respectively. The peak current increased upon successive cycling and it was an indication of the deposition of polymer.

The redox activity of the polymers was tested by CV in ACN containing 0.1 M NaClO₄ at different scan rates. Comparison of the CVs of resulted polymers namely, PIn, PCz, and P[In-co-Cz] is given in Figure 3d. P[In-co-Cz] has a peak potential in between PIn and PCz, as expected.

During electropolymerization of In-Cz comonomers, CVs were obtained and are given in Figure 4. The anodic potential limit of polymerization in all cases was selected as 1.75 V, since 4In-3Cz, comonomer does not polymerize at lower potentials. In order to optimize the polymerization conditions, the same potential range was selected for all monomers. Increase in current intensity was higher in the case of 4In-3Cz and 6In-3Cz than 5In-3Cz and 7In-3Cz and this result suggested that thicker film formation occurred in the case of 4In-3Cz and 6In-3Cz comonomers.

Table 1. E_{ox} and I_p values of monomers.

Monomer	E_{ox} , V	I_p , eV
In	1.14	5.54
Cz	1.24	5.64
[In+Cz]	1.16	5.56
4In-3Cz	1.06	5.46
5In-3Cz	1.19	5.59
6In-3Cz	1.00	5.40
7In-3Cz	1.09	5.49

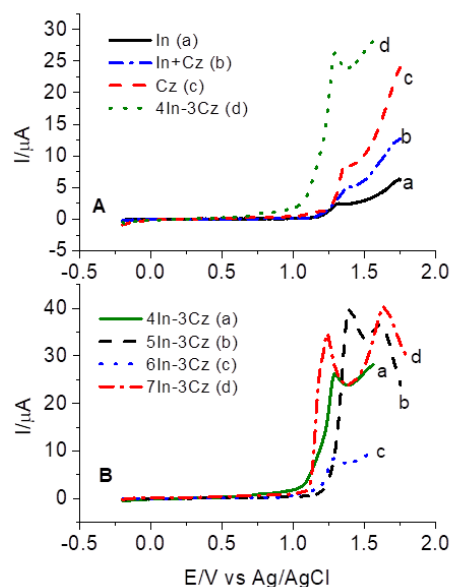


Figure 2. Anodic polarization curves a) In, b) In+Cz mixture, c) Cz, d) 4In-3Cz. (A) and a) 4In-3Cz, b) 5In-3Cz, c) 6In-3Cz, d) 7In-3Cz (B) in ACN containing 0.1 M NaClO₄.

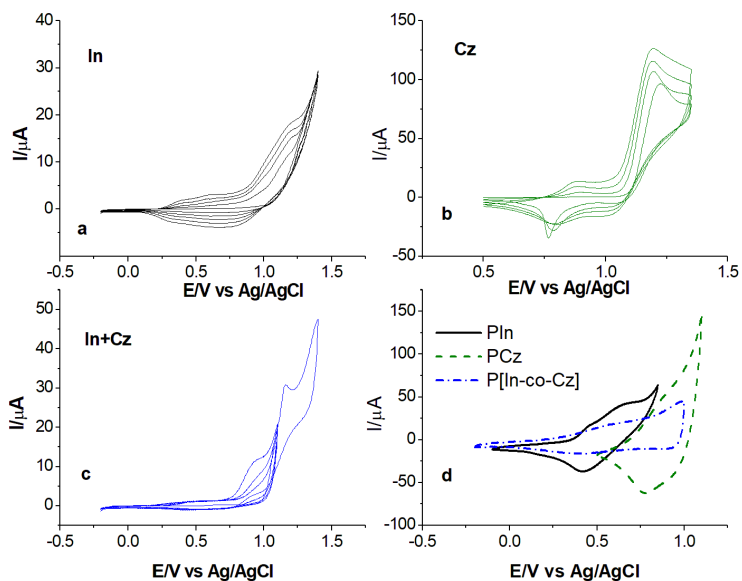


Figure 3. CVs of 1.0×10^{-3} M In (a), 1.0×10^{-3} M Cz (b), and 0.5×10^{-3} In + 0.5×10^{-3} M Cz mixture (c) at 20 mV/s and CV of PIn, PCz and P[In-co-Cz] at scan rate of 200 mV/s (d) in an ACN/ 0.1 M NaClO₄ solution.

The redox behaviors of resulting polymeric films obtained by applying different cycle numbers were compared (Figure 5). For example, for the P[7In-3Cz], the optimum number of cycles was accepted as 4, since the redox behavior of the film obtained by applying 4 cycles was better than the film obtained in 2 and 8 cycles.

Polymerizations were also carried out in different potential ranges for 5In-3Cz, 6In-3Cz, 7In-3Cz. It was found that the redox behavior of polymer depends on the anodic potential limit and at lower potential limit; more electrochemically reversible polymeric films were obtained as expected [49]. This comparison was given for P[7In-3Cz] as an example (Figure 6). As it can be seen the polymer film obtained at the potential limit of 1.75 V has quasireversible redox behavior due to some degradation in the polymer chain.

Scan rate dependence of P[In-Cz]'s is given in Figure 7.

De-doping peak of P[6In-3Cz] was not significant as much as the peaks of P[4In-3Cz], P[5In-3Cz] and P[7In-3Cz]. Generally, CV of conducting polymers demonstrates "irreversible" anodic and cathodic peaks and there are several explanations for such behaviors [50]. Free rotation of the molecule during the transition from benzenoid to quinoid structure might be hindered by deposited oligomers on the electrode as a solid matrix and the typical voltammogram is the superposition of different redox waves, i.e. a mixture of oligomers, and polymers of different chain lengths and possibly different cross-linking. Role of coupling position seems to affect the redox behavior of polymer and superposition of different redox waves became more pronounced at lower scan rates for P[5In-3Cz] and P[7In-3Cz].

The comparison of CVs of all In-Cz polymer films is given in Figure 8a. As it can be seen, although the peak potentials of polymers were close to each other, the highest peak current was observed for P[7In-3Cz]. This result indicated that the coupling position affected the electroactivity of P[In-Cz] films and P[7In-3Cz] seems to be the most electroactive one.

Scan rate dependence on the anodic and cathodic peak currents (I_{pa} and I_{pc}) of P[4In-3Cz], P[5In-3Cz], P[6In-3Cz] and P[7In-3Cz] was investigated comparatively with PIn and PCz obtained under the same experimental condition. It was found that I_{pa} and I_{pc} scale linearly with scan rates not with square root of scan rates and this result indicate an electroactive thin film behavior instead of diffusion control one as suggested in literature [49] (Figure 8b). The order of the current intensities was found as follows: P[7In-3Cz] > PCz > PIn > P[4In-3Cz] > P[6In-3Cz] > P[5In-3Cz].

4.3. FT-IR results

The FT-IR spectra of PIn and PCz, P[In-co-Cz] and P[4In-3Cz] are given in Figure 9. The characteristic vibrations of Cz and indole rings are very similar. Therefore, it is difficult to interpret the coupling position. Two rings give similar vibration at very close wave numbers and when they coupled each other these peaks are split. -C - H out of plane deformation peaks were observed at 739 and 794 cm⁻¹ for PIn, and at 727, 746, and 800 cm⁻¹ for PCz and split into three peaks in the range of

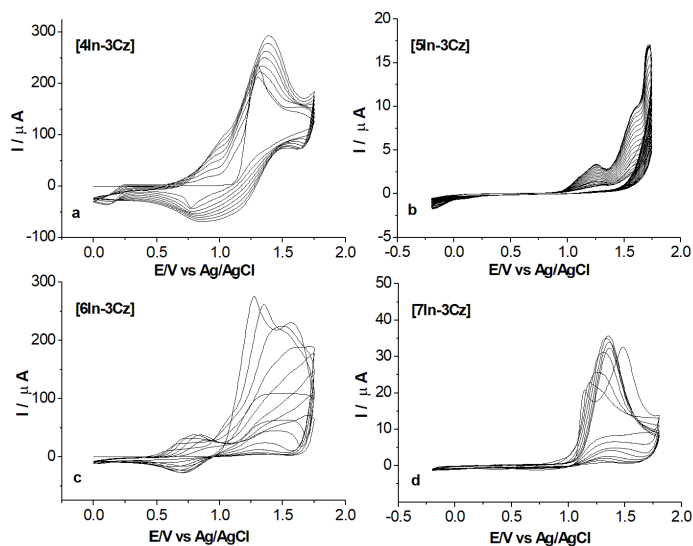


Figure 4. CV of 1.0×10^{-3} M 4In-3Cz (a), 5In-3Cz (b), 6In-3Cz (c) and 7In-3Cz (d) in ACN containing 0.1 M NaClO_4 solution with a scan rate of 20 mV/s.

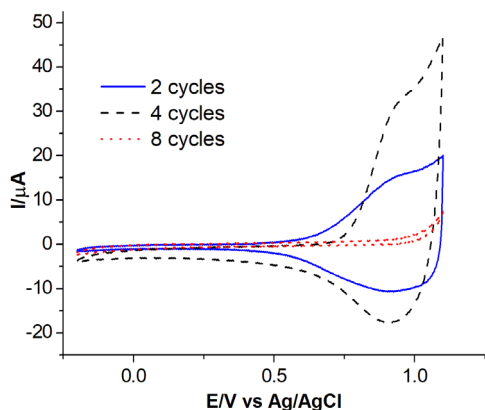


Figure 5. Comparison of cyclic voltammograms of P[7In-3Cz] films obtained by potentiodynamic method by applying 2, 4, and 8 cycles, in ACN containing 0.1 M NaClO_4 . Scan rate: 200 mV/s

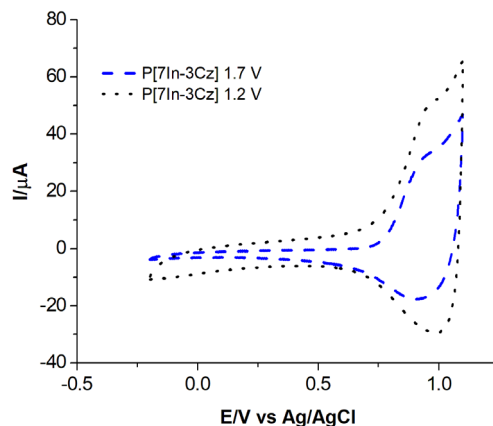


Figure 6. CV of P[7In-3Cz] film obtained potentiodynamically at two different potential ranges (0.0–1.2 V and 0.0–1.7 V).

$810\text{--}734\text{ cm}^{-1}$ in the case of P[4In-3Cz]. This result showed the presence of both In and Cz in the structure of P[4In-3Cz]. The peak at 1400 cm^{-1} , which belongs to the aromatic -C - H vibration, was observed in PCz, but not in PIn, and shifted to 1393 cm^{-1} in the case of P[4In-3Cz]. This result indicates that Cz is included in the structure. Similarly, the presence of the peak at 927 cm^{-1} for PIn but the absence for PCz, observed at 927 cm^{-1} for P[4In-3Cz] showed the inclusion of indole to the P[4In-3Cz] structure. An absorption band at 1100 cm^{-1} which is attributed to ClO_4^- , showed doping of the polymers with this anion (Figure 9). The peak at 740 cm^{-1} corresponding to the out of plane deformation of aromatic -C - H of Cz and indole, was observed with higher intensity for P[In-co-Cz] by splitting in two (745 and 720 cm^{-1}). This indicated less coupling possibility through the benzene ring during the random copolymerization of In and Cz.

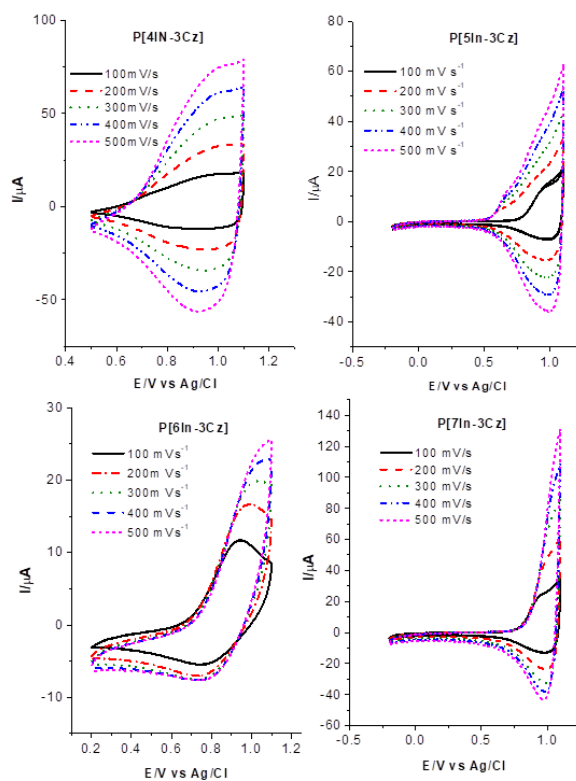


Figure 7. CV of a P[4In-3Cz] (a), P[5In-3Cz] (b), P[6In-3Cz] (c) and P[7In-3Cz] (d) ACN containing 0.1 M NaClO₄ at different scan rates.

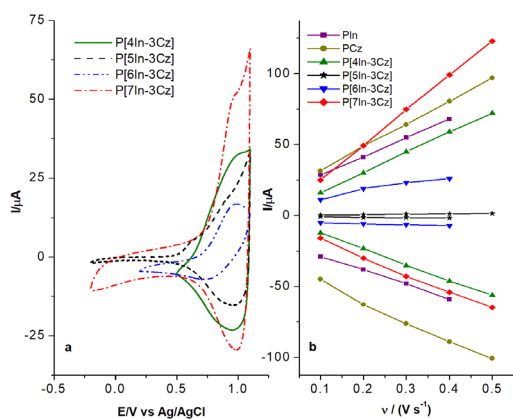


Figure 8. CV of P[4In-3Cz], P[5In-3Cz], P[6In-3Cz], P[7In-3Cz] at a scan rate of 100 mV/s (a) and scan rate dependence of the anodic and cathodic peak currents (b) of polymer films obtained on the Pt electrode.

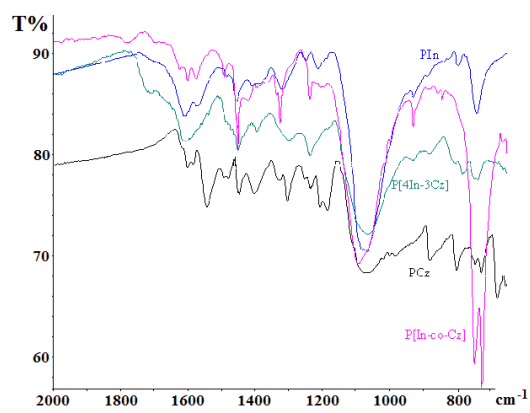


Figure 9. ATR-FTIR spectra of P[In], PCz, P[In-co-Cz] and P[4In-3Cz].

4.4. Optical properties

Spectroelectrochemical methods were also employed to study optical properties of polymers by applying anodic potentials which results polaron and bipolaron formations. P[4In-3Cz], P[5In-3Cz], P[6In-3Cz] and P[7In-3Cz] films were electrochemically polymerized on ITO for spectroelectrochemical analysis and subsequently placed in a quartz cuvette with Pt counter and Ag reference electrodes. For reduction and to obtain their neutral states, -1.0 V was applied to the polymers. UV-visible spectrum of P[4In-3Cz] obtained by applying different potential is shown in Figure 10. The peak at 350 nm was observed it was attributed to π - π^* transition. The new peak at 870 nm was started to form by application of anodic potential at 0.8 V and this might be due to polaron and/or bipolaron formation. As the anodic potential was increased (up to 1.1 V and further), absorption maximum shifted to 700 nm. This might occur by oxidation of polymer chains that results better and less ordered polymer structures as suggested for other PTh derivatives [51-53]. Another explanation might be formation of the segments with different conjugation length [54] and these two approaches are very close to each other.

E_g values of polymers were estimated from UV-visible spectrophotometric measurements, by extrapolation of the low energy edge to the baseline of the spectra and results are given in Table 2. While P[4In-3Cz] and P[6In-3Cz] have lower E_g than PIn and PCz, P[5In-3Cz] has similar value with PIn, and P[7In-3Cz] has the highest E_g . It is found that E_g could be decreased by obtaining polymers from In-Cz comonomer that synthesized by coupling of In and Cz instead of random copolymerization.

E_{ox} of P[In-Cz]s were calculated from the equation (1) above and showed similar trends with comonomers. Results are given in Table 2. It can be seen that E_{ox} of P[In-Cz]s was slightly different from the values of PIn and PCz. E_{ox} and E_g values of conjugated polymers are expected to decrease with the extension of π -conjugation length. When the E_{ox} of polymers and monomers are compared (Table 2), it can be seen that E_{ox} significantly decreases in the case of polymers. Variation in molecular architecture of resulting polymer has different effects on ionization potential and electron transition between the HOMO and LUMO levels; therefore, changes in E_{ox} values were different from variation of E_g values.

4.5. EIS measurements

To explore the capacitive behavior of polymers, EIS measurements were performed and Nyquist diagrams of PIn, PCz, P[In-co-Cz], and P[4In-3Cz] films are given in Figure 11. Specific capacitance values (C_{sp}) were calculated from the slope of imaginary component of the impedance, $-Z_{im}$ versus $1/\text{frequency}$ (f) plot, by using the equation below as suggested in the literature [55] and the results are summarized in Table 2.

$$Z_{im} = \frac{1}{2\pi C_{sp} f}$$

Capacitive behaviors of polymers depend on the structure, and the highest C_{sp} value was obtained in the case of P[4In-3Cz]. This structure seems to be the most favorable one for charge storage applications. The C_{sp} values of the copolymers needed to be improved by changing reaction conditions for application.

Experimental EIS results were analyzed by fitting an equivalent circuit model. Different electrical models were tried and with the one that has the lowest chi-squared value, an excellent agreement between experimental and simulated data was obtained as shown in Figure 12. The values of the circuit elements obtained as a result of the simulation are summarized in the Table 3.

Table 2. The conductivities, I_p , E_g , and C_{sp} of polymers.

Polymer	Conductivity, mS/cm	E_{ox} , V	I_p , eV	E_g , eV	C_{sp} , $\mu\text{F}/\text{cm}^2$
PIn	0.3	0.41	4.81	2.70	1250
PCz	0.7	0.69	5.09	2.55	650
P[In-co-Cz]	0.2	0.55	4.95	2.87	840
P[4In-3Cz]	1.1	0.66	5.06	2.40	630
P[5In-3Cz]	1.0	0.52	4.92	2.16	530
P[6In-3Cz]	2.4	0.72	5.12	2.40	240
P[7In-3Cz]	0.1	0.78	5.18	3.21	110

The value of R_1 in the circuit belongs to the solution resistance of the cell, constant phase elements (CPEs) and R_2 and R_3 belong to the nonideal capacitances and resistances of the polymer film and electrode, respectively, and W to the Warburg element related to mass transfer.

The impedance of a capacitor is obtained by the following equation and the CPE value is used in case of nonideal capacitors account for surface roughness, nonuniform current distribution etc. and the exponent n is less than one:

$$Z_{CPE} = \frac{1}{(j\omega)^n Y_0}$$

where Y_0 is the capacitance, C , and n is an exponent equaling 1 for ideal capacitor

The equation for Warburg impedance and can be written as follows:

$$Z_w = \frac{1}{\sqrt{j\omega} Y_0}$$

where

$$Y_0 = \frac{1}{\sqrt{2}\sigma} \text{ and } \sigma = \frac{RT}{n^2 F^2 A \sqrt{2}} \left(\frac{1}{C_o \sqrt{D_o}} + \frac{1}{C_R \sqrt{D_R}} \right)$$

ω = radial frequency (s^{-1})

D_o = diffusion coefficient of the oxidant (cm^2/s)

D_R = diffusion coefficient of the reductant (cm^2/s)

A = surface area of the electrode (cm^2)

n = number of electrons transferred

Table 3. Impedance parameters of P[4In-3Cz] film obtained from R(Q(R(Q(RW)))) type equivalent circuit model.

Element	R_1 , ohm	CPE, Y_0 S sec ⁿ	n	R_2 , ohm	CPE, Y_0 S sec ⁿ	n	R_3 , ohm	Warburg, Y_0 S sec ⁵	C_{sp}^{EIS} $\mu F/cm^2$	Chi-squared
Value	227.4	6.75×10^{-7}	0.922	89.1	3.44×10^{-7}	0.158	538.5	4.46×10^{-7}	463	7.4×10^{-4}

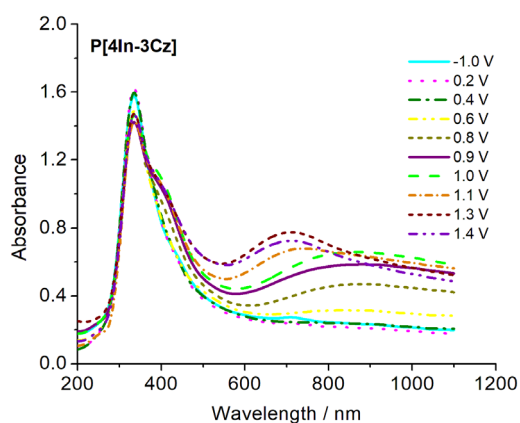


Figure 10. UV-visible absorption spectra of P[4In-3Cz].

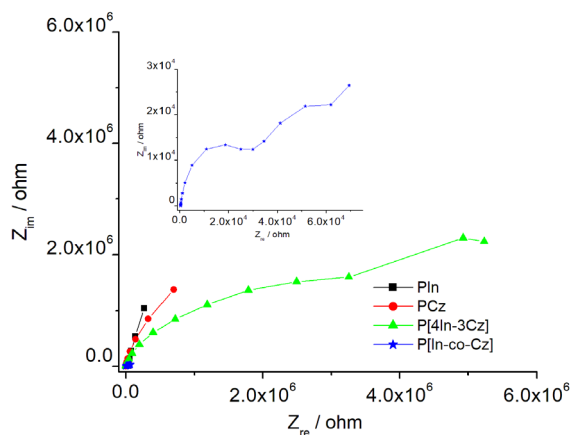


Figure 11. Nyquist diagrams of PIn, PCz, P[In-co-Cz], and P[4In-3Cz] films in the frequency range of 10×10^3 Hz – 10×10^{-3} Hz at open circuit potential. Enlarged Nyquist diagram of P[In-co-Cz] at high frequency region (inset).

C = bulk concentration of the diffusing species (moles/cm³)

Total capacitance, C_{spEIS} , was calculated and is given in Table 3. When experimentally determined and simulated capacitance values were compared, they were found to be in good agreement.

4.5. Conductivity measurements

Electrodeposition leads to a doped and conductive polymer, where the perchlorate ion is the dopant. The solid-state conductivities of the polymer films are given in Table 2.

The conductivity values of the polymers agree with literature and have the expected values in the range for PIn and PCz [1, 56, 62, 63]. The highest conductivity was obtained in the case of P[6In-3Cz]. This could be due to higher conjugation possibility and change in growth behavior of P[6In-3Cz] that affects the inclusion of dopant ion.

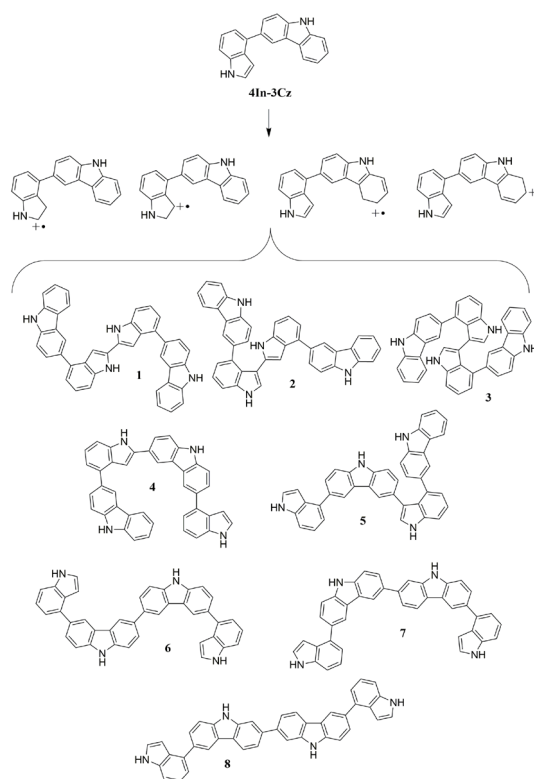
4.6. Possible dimers and tetramers structures of comonomers

E_{ox} , E_g , conductivity, C_{sp} values of copolymers suggested that different structures were obtained by polymerization of comonomers and the mixture of two monomers. Although only random copolymers can be obtained from the mixtures, it is possible to obtain alternated structures by using newly synthesized comonomers which have improved properties. Theoretical and experimental methods were used together in order to have an idea about the relationship between the application-oriented properties of polymers such as E_{ox} , E_g , and C_{sp} .

The possibility of polymerization from 2 and 3 positions of indole [57-61] and 3 position of Cz [62-64] allows the formation of many dimers for each comonomer as given in Scheme 3 due to asymmetric structure of comonomers. Dimers 7 and 8 are less likely to occur during the polymerization since they coupled through the 2 position of Cz.

As it can be seen, by oxidation of 4In-3Cz comonomer cation radicals can be formed which was coupled in the following step and formed 2,3-indole-indole dimer, called $D[2,3(In-In)]_{4In-3Cz}$. The numbers and abbreviation of the name of dimers that may occur from 4In-3Cz cation radicals are summarized in Table 4.

In the propagation step, after oxidation, these dimers can couple with each other and formed tetramers, for instance, $D[2,3(In-In)]_{4In-3Cz}$ can couple through 3,3' position of Cz and give the tetramer named as $T(3,3'(Cz-Cz))_{4In-3Cz}$ (Scheme 4).



Scheme 3. Possible dimers to be formed from the 4In-3Cz comonomer.

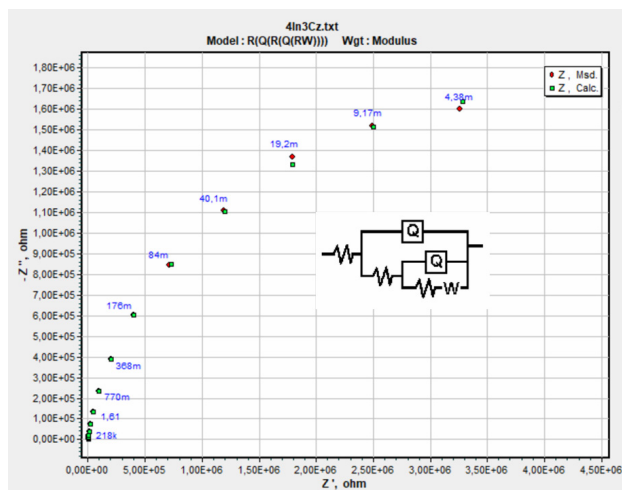
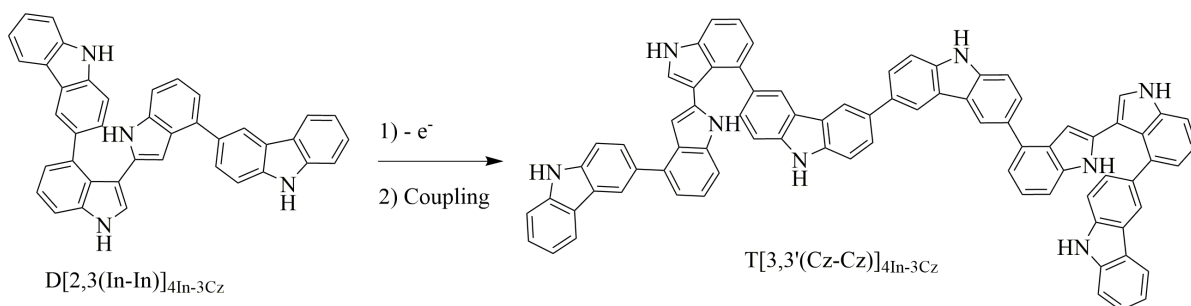


Figure 12. Experimental and simulated Nyquist diagrams of P[4In-3Cz] film with. Equivalent circuit model (inset).

Table 4. The numbers and abbreviation of the name of possible dimers to be formed from the 4In-3Cz comonomer.

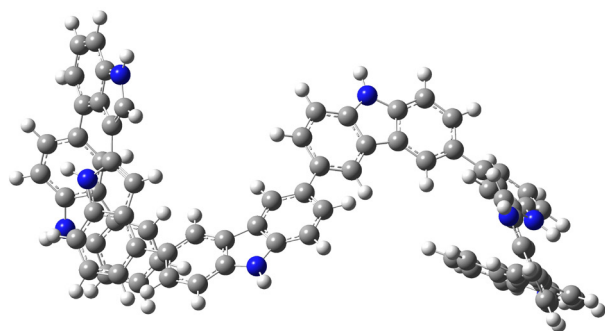
Dimer number	Abbreviation of the name of dimers
1	D[2,2'-(In-In)] _{4In-3Cz}
2	D[2,3-(In-In)] _{4In-3Cz}
3	D[3,3'-(In-In)] _{4In-3Cz}
4	D[2,3-(In-Cz)] _{4In-3Cz}
5	D[3,3'-(In-Cz)] _{4In-3Cz}
6	D[3,3'-(Cz-Cz)] _{4In-3Cz}
7	D[2,3-(Cz-Cz)] _{4In-3Cz}
8	D[2,2'-(Cz-Cz)] _{4In-3Cz}



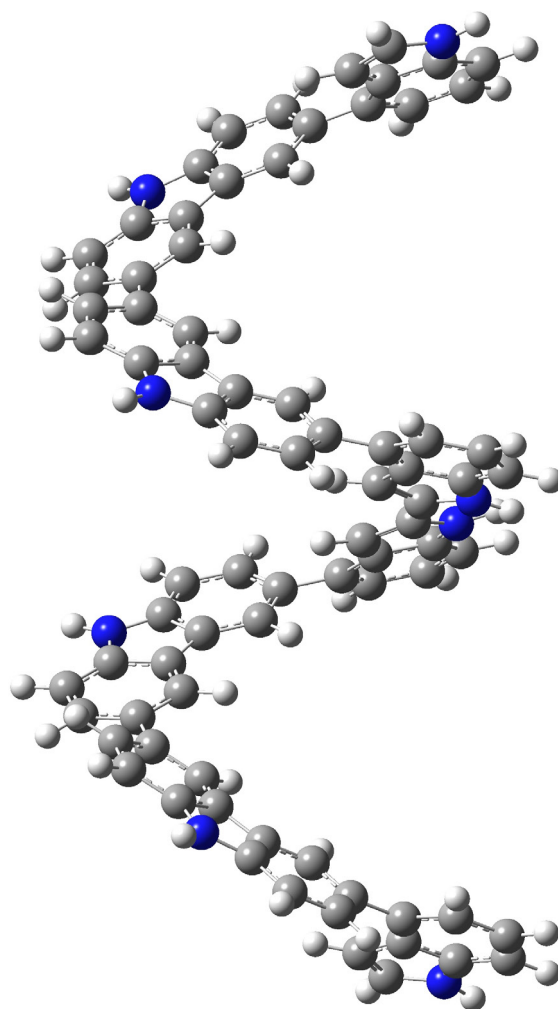
Scheme 4. Coupling steps of the formation of D[2,3(In-In)]_{4In-3Cz} dimer and T[3,3'(Cz-Cz)]_{4In-3Cz} tetramer.

Similarly, other possible dimer structures of 4In-3Cz might be obtained by coupling of Cz cation radicals that formed at the 3 position of Cz rings and called $D[3,3'(Cz-Cz)]_{4In-3Cz}$. Further oxidation of this dimer might result a tetramer by coupling of indole rings through their 2 positions which resulted a tetramer named $T[2,2'(In-In)]_{4In-3Cz}$. Coupling positions have significant role in the properties of resulting copolymers. DFT allowed to resolve the problems concerning the monomer linkage as suggested in the literature for polymerization of 1,8-diaminocarbazole [65]. It would be better to carry out similar calculations to clarify the most probable structures.

Preliminary calculation was carried out for $T(3,3'(Cz-Cz))_{4In-3Cz}$ and $T[2,2'(In-In)]_{4In-3Cz}$ and optimized geometries of them are given in Schemes 5 and 6. As can be seen, the geometry of the tetramer changes significantly as the coupling position changes, and since the electronic properties of polymers are formed by the contribution of all oligomers, it is difficult to make a precise prediction about the mechanism and structure-property relationship without further theoretical investigation



Scheme 5. Optimized geometry of $T(3,3'(Cz-Cz))_{4In-3Cz}$ tetramer formed from $D[2,3(In-In)]_{4In-3Cz}$ dimer.



Scheme 6. Possible optimized geometry of $T[2,2'(In-In)]_{4In-3Cz}$ tetramer that formed from $D[3,3'(Cz-Cz)]_{4In-3Cz}$ dimer.

5. Conclusion

The Stille cross-coupling reaction was applied to obtain various carbazolyindoles and their chemical structures were fully characterized by common techniques.

Although random copolymers can be obtained by polymerization of In and Cz mixture, alternated copolymers have been obtained by using newly synthesized In-Cz comonomers.

In + Cz mixture and In-Cz comonomers were electropolymerized and the important properties of their polymers for applications such as redox potential, conductivity, optical band gap and specific capacitance were investigated comparatively.

The changes of optical and electrical properties of In-Cz copolymers synthesized by different indole derivatives showed the role of coupling position of indole ring with Cz. For example, the higher conductivities were obtained in the case of P[6In-3Cz]. Conductivity depends on the conjugation length and geometries of structure. Therefore, it can be said that P[6In-3Cz] has the most planar geometries and/or the highest conjugation length. The evaluation of the relationship between the chemical structure of copolymers and their specific properties were supported by theoretical calculations.

To obtain an In-Cz copolymer with low oxidation potential and band gap, one must substitute indole ring through 5 to the 3 position of Cz. indicate that it has a more planar conjugation keeping the HOMO-LUMO energy level at the lowest. The specific capacitance values of copolymers were lower than that of homopolymer. P[4In-3Cz] has the highest C_{sp} value among the series and this can be explained by the combination of oligomers formed from the 4In-3Cz comonomer that highly porous structure. In other words, P[4In-3Cz] possessed the most suitable structure for capacitive applications, while P[5In-3Cz] and P[6In-3Cz] were the most favorable candidates for electronic applications.

Acknowledgment

This work was supported in part by the Scientific and Technical Research Council of Turkey (TÜBİTAK) under Project Number: 106T070.

References

1. Morin JF, Leclerc M, Ades D, Siove A. Polycarbazoles: 25 Years of Progress. *Macromolecular Rapid Communication* 2005; 26 (10): 761-778. <https://doi.org/10.1002/marc.200500096>
2. Saraswathi R, Gerard M, Malhotra BD. Characteristics of aqueous polycarbazole batteries. *Journal of Applied Polymer Science* 1999; 74 (1): 145-150. [https://doi.org/10.1002/\(SICI\)1097-4628\(19991003\)74:1<145::AID-APP18>3.0.CO;2-C](https://doi.org/10.1002/(SICI)1097-4628(19991003)74:1<145::AID-APP18>3.0.CO;2-C)
3. Verghese MM, Ram MK., Vardhan H, Malhotra BD, Ashraf SM. Electrochromic properties of polycarbazole films. *Polymer* 1997; 38: 1625. [https://doi.org/10.1016/s0032-3861\(96\)00655-6](https://doi.org/10.1016/s0032-3861(96)00655-6)
4. Sivakkumar SR, Angulakshmi N, Saraswathi R. Characterization of Poly (indole-5-carboxylic Acid) in Aqueous Rechargeable Cells. *Journal of Applied Polymer Science*, 2005; 98: 917.
5. Maarouf EB, Billaud D, Hannecart E. Electrochemical cycling and electrochromic properties of polyindole. *Materials Research Bulletin* 1994; 29 (6): 637.
6. Pandey PC, Prakash R. Electrochemical Cycling and Electrochromic Properties of Polyindole. *Electrochemical Society* 1998; 145 (3): 999.
7. Pandey PC, Prakash R. Characterization of Electropolymerized Polyindole: Application in the Construction of a Solid-State, Ion-Selective Electrode. *Journal Electrochemical Society* 1998; 145 (12): 4103.
8. Machida K, Hiraki R, Takenouchi H, Naoi K. Redox capacitor properties of indole derivatives II. Electrochemical characteristics of substituted cyclic indole trimers. *Electrochemistry* 2005; 73 (9): 813-822.
9. Dündükü M, Udum YA, Ergun Y, Köleli F. Electrodeposition of poly (4-methyl carbazole-3-carboxylic acid) on steel surfaces and corrosion protection of steel. *Journal of Applied Polymer Science* 2009; 111 (3): 1496-1500.
10. Somasundrum M, Bannister JV. Mediatorless electrocatalysis at a conducting polymer electrode: application to ascorbate and NADH measurement. *Journal Chemical Society Chemical Communication* 1993; 21: 1629-1631.
11. Wan F, Li L, Wan X, Xue G. Modification of Polyindole by the incorporation of Pyrrole Unit. *Journal of Applied Polymer Science* 2002; 85 (4): 814-820.
12. Dhanalakshmi K, Saraswathi R. Electrochemical preparation and characterization of conducting copolymers: poly(pyrrole-co-indole). *Journal Material Science* 2001; 36 (17): 4107.

13. Nie G, Han X, Zhang S, Xu, J, Cai T. Electrochemical copolymerization of indole and 3-methylthiophene. *Journal of Applied Polymer Science* 2007; 104: 3129.
14. Xu JK, Nie GM, Zhang SS, Han XJ, Hou J et al. Electrochemical copolymerization of indole and 3, 4-ethylenedioxythiophene. *Journal Material Science* 2005; 40 (11): 2867.
15. Saraç AS, Serantoni M, Tofail SAM, Cunnane VJ. Nanoscale Characterization of Carbazole–Indole Copolymers Modified Carbon Fiber Surfaces. *Journal of Nanoscience and Nanotechnology* 2005; 5 (10): 1677.
16. Kuo CW, Hsieh TH, Hsieh CK, Liao JW, Wu TY. Electrosynthesis and Characterization of Four Electrochromic Polymers Based on Carbazole and Indole-6-Carboxylic Acid and Their Applications in High-Contrast Electrochromic Devices. *Journal of The Electrochemical Society* 2014; 161 (14): D782-D790.
17. Kuo CW, Wu TY, Huang MW. Electrochromic characterizations of copolymers based on 4,4-bis(N-carbazolyl)-1,1-biphenyl and indole-6-carboxylic acid and their applications in electrochromic devices. *Journal of the Taiwan Institute of Chemical Engineers* 2016; 68: 481–488.
18. Hwang J, Park J, Kim YJ, Ha YH, Park CE et al. Indolo[3,2-b]indole-Containing Donor–Acceptor Copolymers for High-Efficiency Organic Solar Cells. *Chemical Materials* 2017; 29 (5): 2135–2140. <https://doi.org/10.1021/acs.chemmater.6b04745>
19. Wadatar NS, Waghuley SA. Electrical investigation on thiophene–indole conducting copolymers as synthesized through in situ chemical copolymerization route. *Polymer Bulletin* 2020; 77: 4181–4196. <https://doi.org/10.1007/s00289-019-02967-w>
20. Katsoulidis AP, Dyar SM, Carmieli R, Malliakas CD, Michael R et al. Copolymerization of terephthalaldehyde with pyrrole, indole and carbazole gives microporous POFs. *Journal of Material Chemistry A*, 2013; 1: 10465-10473.
21. Gobalasingham NS, Ekiz S, Pankow RM, Livi F, Bundgaard E et al. Carbazole-based copolymers via direct arylation polymerization (DARp) for Suzuki-convergent polymer solar cell performance. *Polymer Chemistry* 2017; 8 (30): 4393-402.
22. Xiao H, Deng Y, Yuan J, Gao P, Zhao B et al. Synthesis and Photovoltaic Properties of the Copolymers Based on Carbazole with Tetrathiophene Porphyrin Side Chains Linked by a Flexible Alkyl-interval. *Chinese Journal of Chemistry* 2018; 36 (7): 599-604. <https://doi.org/10.1002/cjoc.201700804>
23. Maertens F, Toppet S, Hoornaert GJ, Compernelle F. Incorporation of an indole-containing diarylbutylamine pharmacophore into furo [2, 3-a] carbazole ring systems. *Tetrahedron* 2005; 61 (7): 1715.
24. Bergman J. Condensation of indole and formaldehyde in the presence of air and sensitizers: A facile synthesis of indolo[3.2-b] carbazole. *Tetrahedron* 1970; 26 (13): 3353.
25. Levesque I, Bertrand PO, Blouin N, Leclerc M, Zecchin S et al. Synthesis and thermoelectric properties of polycarbazole, polyindolocarbazole, and polydiindolocarbazole derivatives. *Chemistry. Materials* 2007; 19: 2128.
26. Stille JK. The Palladium-Catalyzed Cross-Coupling Reactions of Organotin Reagents with Organic Electrophiles *New Synthetic Methods. Angewandte Chemie International Edition in English* 1986; 25: 508.
27. Yamamoto T, Yamamoto A. A novel type of polycondensation of polyhalogenated organic aromatic compounds producing thermostable polyphenylene type polymers promoted by nickel complexes. *Chemistry Letters* 1977; 6 (4): 353-356. <https://doi.org/10.1246/cl.1977.353>
28. Heywang G, Jonas F. Poly (alkylenedioxythiophene)-new, very stable conducting polymers *Advanced Material* 1992; 4 (2): 116-118. <https://doi.org/10.1002/adma.19920040213>
29. Faid K, Cloutier R, Leclerc M. Design of novel electroactive polybithiophene derivatives. *Macromolecules* 1993; 26: 2501-2507.
30. Faid K, Frechette M, Ranger M, Mazerolle L, Levesque I et al. Chromic Phenomena in Regioregular and Non-regioregular Polythiophene Derivatives. *Chemistry Materials* 1995; 7: 1390.
31. Leclerc M, Faid K. Electrical and optical properties of processable polythiophene derivatives: structure-property relationships. *Advanced Materials* 1997; 9: 1087.
32. McCullough RD. The chemistry of conducting polythiophenes. *Advanced Materials* 1998; 10: 93.
33. Rehahn M, Schluter AD, Wegner G, Feast WJ. Soluble poly (para-phenylene)s. 1. Extension of the Yamamoto synthesis to dibromobenzenes substituted with flexible side chains *Polymer* 1989; 30: 1054.
34. Pei Q, Yang Y. Efficient photoluminescence and electroluminescence from a soluble polyfluorene. *Journal of American Chemical Society* 1996; 118: 7416.
35. Sotzing GA, Reynolds JR. Electrochromic conducting polymers via electrochemical polymerization of bis (2-(3, 4-ethylenedioxy) thienyl) monomers. *Chemistry Materials* 1996; 8: 882.
36. Geissler U, Hallensleben ML, Rohde N. Poly[arylene-alt-[bis(1-methylpyrrolylene)]s, 1. Synthesis and electrochemical polymerization of terarenes. *Macromolecular Chemistry and Physics* 1996; 197: 2565. <https://doi.org/10.1002/macp.1996.021970819>

37. Sezer E, Hooren M Van, Saraç AS, Hallensleben ML. Synthesis and electrochemical polymerization of ter-arenes based on N-ethyl carbazole and thiophene. *Journal of Polymer Science Part A Polymer Chemistry* 1999; 37: 379. [https://doi.org/10.1002/\(SICI\)1099-0518\(19990215\)37:4<379::AID-POLA1>3.0.CO;2-I](https://doi.org/10.1002/(SICI)1099-0518(19990215)37:4<379::AID-POLA1>3.0.CO;2-I)
38. Sezer E, Saraç AS, Parlak EA. Electrochemical synthesis of EDOT–ECZ–EDOT copolymer on carbon fiber micro-electrodes. *Journal of Applied Electrochemistry* 2003; 33: 1233.
39. Saraç AS, Sarioğlan SÖ, Dziomba T, Sezer E. Synthesis and electrocoating of indole–thiophene comonomer on carbon fiber microelectrode, and surface topography by AFM. *European Polymer Journal* 2007; 43: 3392.
40. Cebeci FÇ, Sezer E, Saraç AS. Synthesis and electrochemical characterization of bis (3,4-ethylene-dioxythiophene)-(4,4'-dinonyl-2,2'-bithiazole) comonomer. *Electrochimica Acta* 2007; 52: 2158.
41. Sezer E, Heinze J. Voltammetric, EQCM, and in situ conductivity studies of 3, 6-bis (2-thienyl)-N-ethyl carbazole. *Electrochimica Acta*, 2006; 51: 3668.
42. Roncali J. Conjugated poly (thiophenes): synthesis, functionalization, and applications. *Chemical Reviews* 1992; 92: 711-738.
43. Bergman J. Synthesis of 3-substituted indoles starting from isatin. *Acta Chimica Scandinavica* 1971; 25: 4.
44. Benhida R, Lecubin F, Fourrey JL, Castellanos LR, Quintero L. Synthesis of 6-allyl and 6-heteroarylindoles by palladium catalysed Stille cross-coupling reaction. *Tetrahedron Letters* 1999; 40: 5701.
45. ASTM F42-93; Standard Test Methods for Conductivity Type of Extrinsic Semiconducting Materials. Annual Book ASTM Standard 1997. Last Updated: Aug 16, 2017.
46. Keithley Application Note Series. Measuring the Resistivity and Determining the Conductivity Type of Semiconductor Materials Using a Four-Point Collinear Probe and the Model 6221 DC and AC Current 2005; Source Number 2615.
47. Frisch MJ, Trucks GW, Schlegel HB, Scuseria GE, Robb MA et al., Gaussian 03, Gaussian Inc., Pittsburgh PA, Revision 2003: B:04.
48. Janietz S, Bradley DDC, Grell MM, Giebeler C, Inbasekaran M et al. Electrochemical determination of the ionization potential and electron affinity of poly (9, 9-dioctylfluorene) *Applied Physical Letter* 1998; 73 (17): 2453.
49. Vorotyntsev MA, Zinovyeva VA, Konev DV. Mechanisms of Electropolymerization and Redox Activity: Fundamental Aspects, in: *Electropolymerization: Concepts, Materials and Applications*, Cosnier S, Karyakin AA (Editors). Weinheim, Germany: Wiley-VCH, 2010, pp.27–50.
50. Nalwa HS. (Ed.), *Handbook of Organic Conductive Molecules and Polymer*, John Wiley: New York, 1997, V2, pp.157.
51. Skompska M, Szkurlat A. The influence of the structural defects and microscopic aggregation of poly (3-alkylthiophenes) on electrochemical and optical properties of the polymer films. *Electrochimica Acta* 2001; 46: 4007.
52. Jiang X, Harima Y, Yamashita K, Tada Y, Ohshita J et al. Doping-induced change of carrier mobilities in poly (3-hexylthiophene) films with different stacking structures. *Chemistry and Physics Letters* 2002; 364: 616.
53. Jiang X, Patil R, Harima Y, Ohsita J, Kunai A. Influences of self-assembled structure on mobilities of charge carriers in π -conjugated polymers. *Journal Physics Chemistry B* 2005; 109: 221.
54. Visy C, Lukkari J, Kankare J. A thermodynamic approach to the interpretation of anodic and cathodic doping of poly (3-methylthiophene). *Journal Electroanalytical Chemistry* 1991; 319: 85.
55. Girija TC, Sangaranarayanan MV. Investigation of polyaniline-coated stainless-steel electrodes for electrochemical supercapacitors. *Synthetic Metals* 2006; 156 (2-4): 244-250.
56. Waltman RJ, Diaz AF, Bargon J. Substituent Effects in the Electropolymerization of Aromatic Heterocyclic Compound *Journal of Physical Chemistry* 1984; 88 (19): 4343-4346.
57. Jackowska K, Kudelski A, Bukowska J. Spectroelectrochemical and EPR determination of the number of electrons transferred in redox process in electroactive polymers polyindole films. *Electrochimica Acta* 1994; 39 (10): 1365-1368.
58. Talbi H, Monard G, Loos M, Billaud D. Theoretical study of indole polymerization. *Journal of Molecular Structure: Theochem* 1998; 434: 129-134.
59. Talbi H, Monard G, Loos M., Billaud D. Theoretical investigation of the monomer reactivity in polyindole derivatives. *Synthetic Metals* 1999; 101: 115-116.
60. Dubnikova F, Lifshitz A. Isomerization of indole. Quantum chemical calculations and kinetic modelling. *Journal Physical Chemistry A* 2001; 105: 3605-3614.
61. Yurtsever M, Yurtsever E. A DFT study of polymerization mechanism of indole. *Polymer* 2002; 43; 6019-6025.

62. Saraç AS, Sezer E, Ustamehmetoğlu B. Oxidative polymerization of N-substituted carbazoles. *Polymer Advanced Technologies* 1997; 8 (9): 556-562.
63. Waltman RJ, Bargon J. Electrically conducting polymers: a review of the electropolymerization reaction, of the effects of chemical structure on polymer film properties, and of applications. *Canadian Journal Chemistry* 1986; 64: 76.
64. Skotheim TA. *Handbook of Conducting Polymers*; Marcel Dekker Inc. New York, 1986.
65. Agata T, Cybulski H, Chmielewski MJ, Bukowska J, Skompska M. Electrochemical and spectroscopic characterization of poly(1,8-diaminocarbazole): Part I. Electropolymerization and determination of the polymer structure by FTIR studies and DFT calculations. *Electrochimica Acta* 2009; 54: 4743.